CrossMark click for updates

Partial loss of TDP-43 function causes phenotypes of amyotrophic lateral sclerosis

Chunxing Yang[a], Hongyan Wang[a], Tao Qiao[a], Bin Yang[a,1], Leonardo Aliaga[b], Linghua Qiu[a], Weijia Tan[a], Johnny Salameh[c], Diane M. McKenna-Yasek[c], Thomas Smith[d], Lingtao Peng[a,e], Melissa J. Moore[a,e,f], Robert H. Brown, Jr.[c], Huaibin Cai[b], and Zuoshang Xu[a,e,g,h,2]

Departments of [a]Biochemistry and Molecular Pharmacology, [c]Neurology, [d]Pathology, and [g]Cell Biology, [e]RNA Therapeutic Institute, [f]Howard Hughes Medical Institute, and [h]Neuroscience Program, University of Massachusetts Medical School, Worcester, MA 01605; and [b]Transgenics Section, Laboratory of Neurogenetics, National Institute on Aging, National Institutes of Health, Bethesda, MD 20892

Edited by Gregory A. Petsko, Weill Cornell Medical College, New York, NY, and approved February 11, 2014 (received for review December 6, 2013)

Amyotrophic lateral sclerosis (ALS) is a fatal neurological disease that causes motor neuron degeneration, progressive motor dysfunction, paralysis, and death. Although multiple causes have been identified for this disease, >95% of ALS cases show aggregation of transactive response DNA binding protein (TDP-43) accompanied by its nuclear depletion. Therefore, the TDP-43 pathology may be a converging point in the pathogenesis that originates from various initial triggers. The aggregation is thought to result from TDP-43 misfolding, which could generate cellular toxicity. However, the aggregation as well as the nuclear depletion could also lead to a partial loss of TDP-43 function or TDP-43 dysfunction. To investigate the impact of TDP-43 dysfunction, we generated a transgenic mouse model for a partial loss of TDP-43 function using transgenic RNAi. These mice show ubiquitous transgene expression and TDP-43 knockdown in both the periphery and the central nervous system (CNS). Strikingly, these mice develop progressive neurodegeneration prominently in cortical layer V and spinal ventral horn, motor dysfunction, paralysis, and death. Furthermore, examination of splicing patterns of TDP-43 target genes in human ALS revealed changes consistent with TDP-43 dysfunction. These results suggest that the CNS, particularly motor neurons, possess a heightened vulnerability to TDP-43 dysfunction. Additionally, because TDP-43 knockdown predominantly occur in astrocytes in the spinal cord of these mice, our results suggest that TDP-43 dysfunction in astrocytes is an important driver for motor neuron degeneration and clinical phenotypes of ALS.

FTD | FTLD | neurodegenerative disease | noncell autonomous toxicity | Lou Gehrig's disease

Transactive response DNA binding protein (TDP-43) is a heterogeneous nuclear RNA binding protein that functions in multiprotein/RNA complexes (1–4). It plays roles in regulating gene expression, including RNA transcription, splicing, transport, and translation (5, 6). Missense mutations in the TDP-43 gene cause TDP-43 aggregation in ∼1–5% of familial ALS (FALS) that comprises ∼10% of total ALS cases (7–9). However, the wild-type protein also forms aggregation in >95% of ALS, including all of the sporadic and the majority of the familial cases (6, 10). Additionally, TDP-43 aggregation is observed in ∼45% of frontotemporal lobar degeneration (FTLD) cases and a significant fraction in cases of other neurodegenerative diseases, including Alzheimer's disease, Parkinson disease, Huntington disease, and chronic traumatic brain injury (10, 11). Because TDP-43 proteinopathy generally accompanies its nuclear depletion, whether a gain of toxicity or a loss of TDP-43 function is involved in neurodegeneration is under debate (9, 12–14).

Some evidence suggests that TDP-43 causes neurodegeneration by a gain of toxicity. Overexpression of both mutant and wild-type TDP-43 can cause neurodegeneration in vitro and in vivo (9, 15), suggesting that an amplification of wild-type TDP-43 function can be toxic. Recent studies suggest that TDP-43 levels are elevated in familial and sporadic ALS cases (16, 17). Furthermore, ALS-linked TDP-43 mutants enhance the stability of TDP-43, consistent with the possibility that TDP-43 mutants mediate their toxicity by increasing the TDP-43 levels (1, 18). One possible source of toxicity may be from protein aggregation, as has been suggested for neurodegenerative diseases in general (19). TDP-43 is prone to aggregate, and ALS-linked mutants have a further elevated aggregation propensity (20–22). TDP-43 aggregation has been observed in some in vitro and in vivo models and is a hallmark in human ALS and FTLD (19). However, direct evidence that these TDP-43 aggregates cause neurodegeneration has not yet been established. Some models show little or no TDP-43 aggregation, yet neurodegeneration still occurs (23–25). Other studies have shown no connection between TDP-43 aggregation and degenerative phenotypes (26, 27).

Some evidence suggests that a loss of TDP-43 function causes neurodegeneration. TDP-43 is normally enriched in the cell nucleus. However, in cells with TDP-43 aggregation, TDP-43 is depleted from the nuclei (10, 28, 29). Because both nuclear depletion and cytoplasmic aggregation are expected to reduce the amount of functional TDP-43, dysfunction of TDP-43 is probable in these cells. Assays of TDP-43 function derived from human CNS tissue implicate the existence of TDP-43 dysfunction in both ALS and FTLD (30, 31). The consequences of TDP-43 dysfunction may be serious. In vitro studies have shown that TDP-43 knockdown can cause defects in neuronal morphology and function

Significance

Amyotrophic lateral sclerosis (ALS) is an incurable neurodegenerative disease that causes paralysis and death. TDP-43 is a protein that regulates gene expression. TDP-43 aggregation and depletion from cell nucleus are found in ALS. Therefore, TDP-43 may cause neurodegeneration by generating toxicity from its aggregation or by a loss of its function. Our experiments test the consequence of a partial loss of TDP-43 function in mice. The results demonstrate that a partial loss of TDP-43 function is sufficient to cause neurodegeneration and ALS symptoms. In addition, we have found evidence for TDP-43 dysfunction in human ALS. Therefore, we propose that TDP-43 dysfunction causes neurodegeneration in the human disease, and future therapy should aim to restore the normal function of TDP-43.

Author contributions: C.Y. and Z.X. designed research; C.Y., H.W., T.Q., B.Y., L.A., L.Q., W.T., J.S., D.M.M.-Y., T.S., L.P., R.H.B., and H.C. performed research; D.M.M.-Y., L.P., M.J.M., R.H.B., and H.C. contributed new reagents/analytic tools; C.Y., H.W., T.Q., B.Y., L.A., L.Q., W.T., J.S., T.S., L.P., M.J.M., H.C., and Z.X. analyzed data; and C.Y. and Z.X. wrote the paper.

The authors declare no conflict of interest.

This article is a PNAS Direct Submission.

[1]Present address: Division of Biology, California Institute of Technology, Pasadena, CA 91125.

[2]To whom correspondence should be addressed. E-mail: zuoshang.xu@umassmed.edu.

This article contains supporting information online at www.pnas.org/lookup/suppl/doi:10.1073/pnas.1322641111/-/DCSupplemental.

and even cell death (21, 32, 33). Loss-of-function models in invertebrates and zebrafish have shown a wide range of defects, ranging from embryonic lethality to morphological and functional defects of the nervous system, vascular system, and muscle degeneration (27, 31, 34–37). In mammalian species, TDP-43 gene deletion leads to early embryonic lethality (38–41). Knockdown or knockout of TDP-43 in mammalian cells in vitro and in vivo also causes degenerative changes and cell death in some cases (21, 33, 38, 42, 43). Thus, the evidence suggests that TDP-43 dysfunction can lead to cellular dysfunction, degeneration, and death.

To further model TDP-43 dysfunction in vivo, a partial loss of function in mammalian species is desirable because it mimics the dysfunction but not a complete loss of function in the diseases. Additionally, experiments from selective knockout of TDP-43 in motor neurons have generated contradictory results, and it is not clear whether a lack of TDP-43 function in motor neuron alone is sufficient to cause motor neuron death (42, 43). Importantly, the motor neuron-selective knockout models do not address the possible contribution of TDP-43 dysfunction in glial cells. Given the fact that TDP-43 aggregation and nuclear depletion also occur in glial cells in human patients (10, 28, 29), TDP-43 dysfunction in glial cells may contribute to motor neuron toxicity and death. To address these questions, we created a transgenic (Tg) mouse line that expressed an artificial microRNA (amiRNA) targeting the TDP-43 mRNA (amiR-TDP43) for knockdown. We demonstrate that the transgene was expressed ubiquitously in both peripheral and CNS tissues. Strikingly, despite the widespread TDP-43 knockdown in various tissue and cell types, these mice predominantly developed age-dependent neurological symptoms, including hyperactivity, weakness, paralysis, and death. Concomitantly, pathological analysis revealed prominent degeneration of layer V cortical neurons and spinal motor neurons. These data suggest that motor neurons possess a heightened vulnerability to TDP-43 dysfunction. Because the transgene was expressed in both neurons and glia and mediated TDP-43 knockdown, our data also suggest that TDP-43 dysfunction in glia facilitates motor neuron degeneration. Finally, to determine whether TDP-43 dysfunction occurs in human ALS, we assayed alternative splicing of TDP-43–regulated genes and detected changes consistent with TDP-43 dysfunction. Our results support the hypothesis that TDP-43 dysfunction in both neurons and glia contributes to the neurodegeneration in ALS.

Results

Expression of an amiR-TDP43 Leads to ALS Phenotypes in Mice. We constructed Tg mice that expressed amiR-TDP43 using a Cre–loxP conditional expression strategy, which would permit temporal and spatial control of TDP-43 knockdown. The construct (amiR–TDP43u) would initially express GFP, but would switch to expressing a red fluorescent protein (RFP) and the amiR-TDP43 upon induction with Cre (44) (*SI Appendix*, Fig. S1*A*). However, although widely used in the literature, this strategy carried a technical artifact and caused microcephaly when we attempted CNS-restricted induction of RFP and the amiRNA (45) (*SI Appendix*, Tables S1 and S2). Our previous studies have shown that this artifact was derived from tandem integration of inverted loxP-containing transgene copies into the genome (*SI Appendix*, Fig. S1*B*), which led to aberrant chromosome segregation (*SI Appendix*, Fig. S1*C*) and death of proliferating cells during brain development (45). Because of this artifact, we were precluded from inducing the transgene expression selectively in the CNS. To circumvent this problem, we crossed the amiR–TDP43u mice with a germ-line inducer, CMV–Cre, and converted the conditional-expression Tg mouse lines to the constitutive-expression ones, which expressed RFP and amiR–TDP43 constitutively and ubiquitously in a Cre-independent manner (*SI Appendix*, Figs. S1*D*, S2, and S6).

The converted line (amiR–TDP43i) expressed RFP, but no GFP, in the brain and spinal cord (*SI Appendix*, Fig. S2 *B–D*) and consistently displayed age-dependent, progressive neurological phenotypes (Fig. 1). The mice initially behaved similarly to their nontransgenic (nTg) littermates but then developed head bobbing, unsteady gait, and discoordinated movements (Movies S1 and S2). Beginning at 4 wk of age, these mice displayed hyperactivity (Fig. 1*A*). However, the hyperactivity was transitory, peaking at ∼5 wk and ending at ∼10 wk of age, after which the mice became progressively weaker and less active compared with their nTg littermates (Movies S1 and S2 and Fig. 1*A*). Also, from ∼5 wk of age, the amiR–TDP43i mice started losing body weight (Fig. 1*B*) and showed reduced vertical behaviors (Fig. 1*C*). These abnormalities were progressive and eventually led to paralysis (Fig. 1*D* and Movies S1 and S2) and death (Fig. 1*E*). The motor weakness and paralysis suggested the presence of muscle denervation. Indeed, needle electromyography (EMG) revealed that the amiR–TDP43i mice developed progressive active denervation of muscles, as indicated by the presence of positive sharp waves (Fig. 1*F* and *SI Appendix*, Table S3). Notably, none of these abnormalities were observed in the parent, uninduced line (amiR–TDP43u) that expressed GFP. The amiR–TDP43u mice showed behavior and survival that were indistinguishable from their wild-type littermates, thus indicating that the phenotypes in the amiR–TDP43i mice were derived from the transgene induction and not from the transgene insertion into the mouse genome.

The amiR–TDP43i mice displayed three end-stage phenotypes: hindlimb paralysis, sudden death, and whole-body paralysis (*SI Appendix*, Tables S4 and S5). The mice that died with hindlimb paralysis were mostly males and had a relatively short lifespan (*SI Appendix*, Tables S4 and S5). Some developed hindlimb paralysis shortly after weaning. Some survived longer and went through a period of hyperactivity and weight loss before hindlimb paralysis (Movie S1 and Fig. 1). The mice with sudden death were also mostly males, which did not have significant weight loss but died suddenly and unpredictably. These mice also had relatively short lifespans (*SI Appendix*, Tables S4 and S5). A possible cause of death in these mice was cardiac failure because many Tg mice had an enlarged heart with TDP-43 knockdown (*SI Appendix*, Fig. S3). The mice with whole-body paralysis survived the longest among the three death phenotypes (*SI Appendix*, Table S5). This group had a stereotypic pattern of progression beginning with hyperactivity (Fig. 1*A*) and weight loss (Fig. 1*B*) before becoming totally paralyzed (Movie S2). A majority of both males and females had this phenotype (*SI Appendix*, Table S4). The average lifespan was slightly shorter in the males than in the females, but the difference was not statistically significant (Fig. 1*E* and *SI Appendix*, Table S5).

As a control, we also generated a line of Tg mice that constitutively expressed a scrambled amiRNA (amiR-SCR) using the same construct design and the same strategy to convert from the GFP-expressing parent line to the constitutive RFP-expressing and amiR-SCR–expressing line (45). Western blot analysis revealed that these Tg mice expressed a higher level of transgene than the amiR–TDP43 mice in the CNS (*SI Appendix*, Fig. S4*A*). However, the amiR-SCR mice did not develop any overt phenotypes up to >700 d of age, and there were no measurable changes in their behavior up to 10 mo of age (*SI Appendix*, Fig. S4 *B* and *C*). Thus, it is unlikely that the expression of RFP and/or an exogenous miRNA nonspecifically caused the neurological phenotypes in the amiR–TDP43i mice. Rather, the phenotypes were likely linked to amiR–TDP43 expression and TDP-43 knockdown.

The Transgenes RFP and amiR–TDP43 Are Expressed in Multiple Tissues and in both Neurons and Glia in the CNS. To verify the TDP-43 knockdown, we first examined the transgene expression. We stained the mouse brain for the RFP distribution and found that

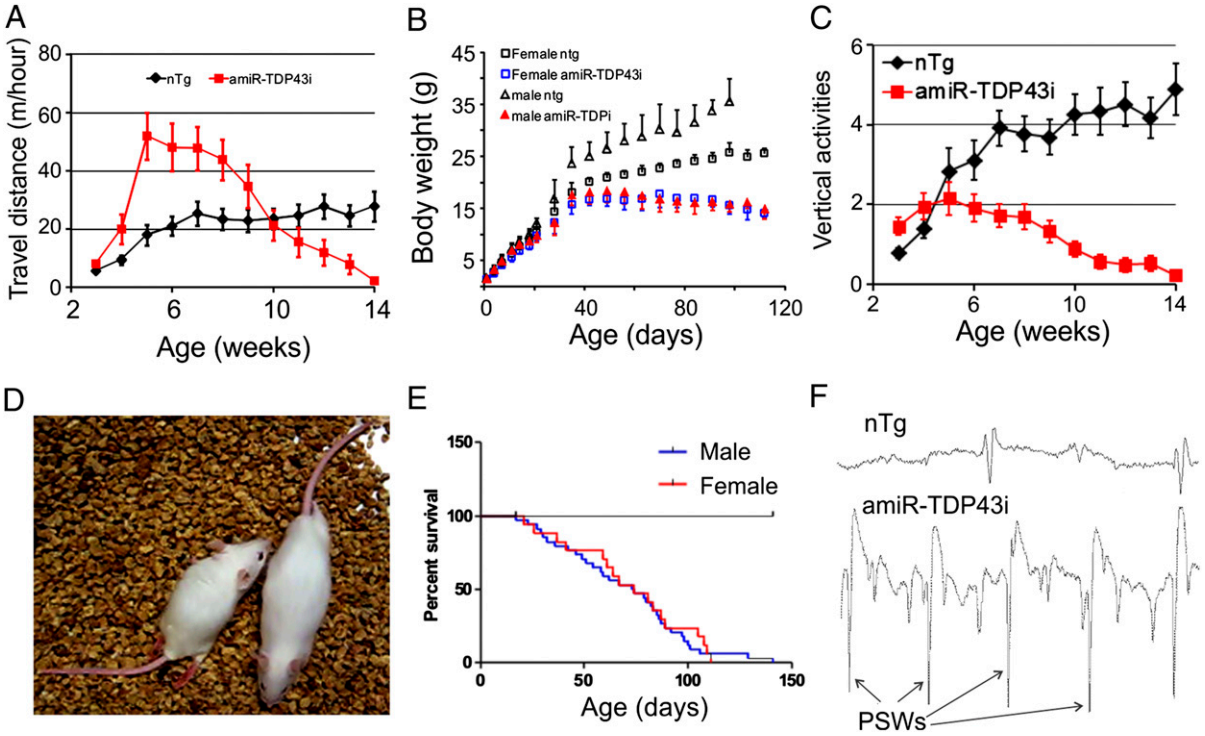

Fig. 1. The amiR–TDP43i mice developed progressive neurological phenotypes. (*A*) The amiR–TDP43i mice went through a hyperactive stage before developing weakness and paralysis. (*B*) The body weight of the amiR–TDP43i mice peaked at ∼50 d of age and then declined until the end stage of the disease. The values were averaged from 7 to 39 animals per group. (*C*) The amiR–TDP43i mice developed weak vertical activities, including rearing and jumping. These activities peaked at 5 wk of age and became progressively weaker thereafter. (*D*) An example of an amiR–TDP43i mouse with hindlimb paralysis. The mouse on the right was an nTg mouse, which was walking past the paralyzed amiR-TDP43i mouse on the left. (*E*) The amiR–TDP43i mice died prematurely (also see *SI Appendix*, Table S5). (*F*) EMG measurement showed a pattern of muscle denervation, as indicated by the presence of positive sharp waves (PSWs; also see *SI Appendix*, Table S3). The data in *A* and *C* were obtained by using a home cage scan system (*SI Appendix*, *SI Materials and Methods*) and from 16 nTg and 19 amiR–TDP43i mice. Both sexes were grouped together because there was no obvious difference in the pattern of progression in these behavioral parameters between the sexes.

the transgene was expressed broadly in the CNS, including forebrain, cerebellum, brainstem, and spinal cord (*SI Appendix*, Fig. S5). Additionally, Western blot analysis for RFP revealed that the transgene was expressed broadly in all tissues and particularly strongly in heart, muscle, and liver (*SI Appendix*, Fig. S6*A*). Furthermore, Northern blot analysis revealed similar pattern of expression for the amiR–TDP43 (*SI Appendix*, Fig. S6*B*). However, the difference in the amiR–TDP43 levels between the periphery and the CNS was not as wide as in the RFP levels (*SI Appendix*, Fig. S6*C*). Nevertheless, both RFP and amiR–TDP43 were expressed at higher levels in the peripheral tissues than in the CNS. This contrasts with the predominant neurological phenotypes in these mice and suggests that the CNS possesses a heightened vulnerability to the effects of the transgene expression.

To determine which CNS cell types express the transgene, we conducted double immunofluorescence analysis. The RFP was expressed in various neuronal types, including cortical neurons, cerebellar Purkinje cells, and spinal cord motor neurons. In addition, the RFP was expressed abundantly in astrocytes and in some oligodendrocytes, but not in microglia (*SI Appendix*, Fig. S7).

amiR–TDP43 Reduces TDP-43 Expression and Function in the CNS. Next we investigated TDP-43 knockdown by measuring TDP-43 levels and function. By bulk protein and mRNA measurements, we observed that TDP-43 was knocked down to modest degrees in the CNS but with large variations among individual animals (Fig. 2 *A*–*C* and *SI Appendix*, Table S6). These variations might be caused by a variable number of cells that expressed transgene in different individual animals. We therefore sorted RFP-positive cells using fluorescence-activated cell sorting and found that only a small percentage of the cells from the cortex and the spinal cord were sorted as RFP-positive cells (Fig. 2*D*), where we detected a robust knockdown of TDP-43 mRNA (Fig. 2*E*). However, we also detected lower TDP-43 levels in RFP-negative cell populations (Fig. 2*E*). This suggested that the cell sorting could only separate the brightest RFP-positive cells, and the cells with modest levels of RFP were left with the RFP-negative cells. To test this possibility, we carried out immunofluorescence staining, which showed that ∼30–50% of cells in the cortex were RFP-positive. These cells showed both neuronal and astrocytic morphology (Fig. 2*F*). In the RFP-positive cells, we detected a decrease in TDP-43 staining intensity compared with the neighboring RFP-negative cells (Fig. 2*G*). Thus, TDP-43 knockdown is correlated with the transgene expression.

To determine whether the TDP-43 knockdown compromised TDP-43 function, we examined changes in alternative splicing in genes that are regulated by TDP-43 (46–48). By PCR across the alternatively spiced exons, we detected the changes known to be caused by TDP-43 knockdown in sorted RFP-positive cells (Fig. 2 *H* and *I*). Additionally, we consistently detected the change in alternative splicing of S6K1 Aly/REF-like target (*Skar*), also known as polymerase delta interacting protein 3 (*Poldip3*), in the CNS homogenates from amiR–TDP43i mice by both RT-PCR from the total RNA and Western blots of total proteins. Specifically, the exon 3-excluded isoform was increased in the brain and spinal cord homogenates (Fig. 2*J*).

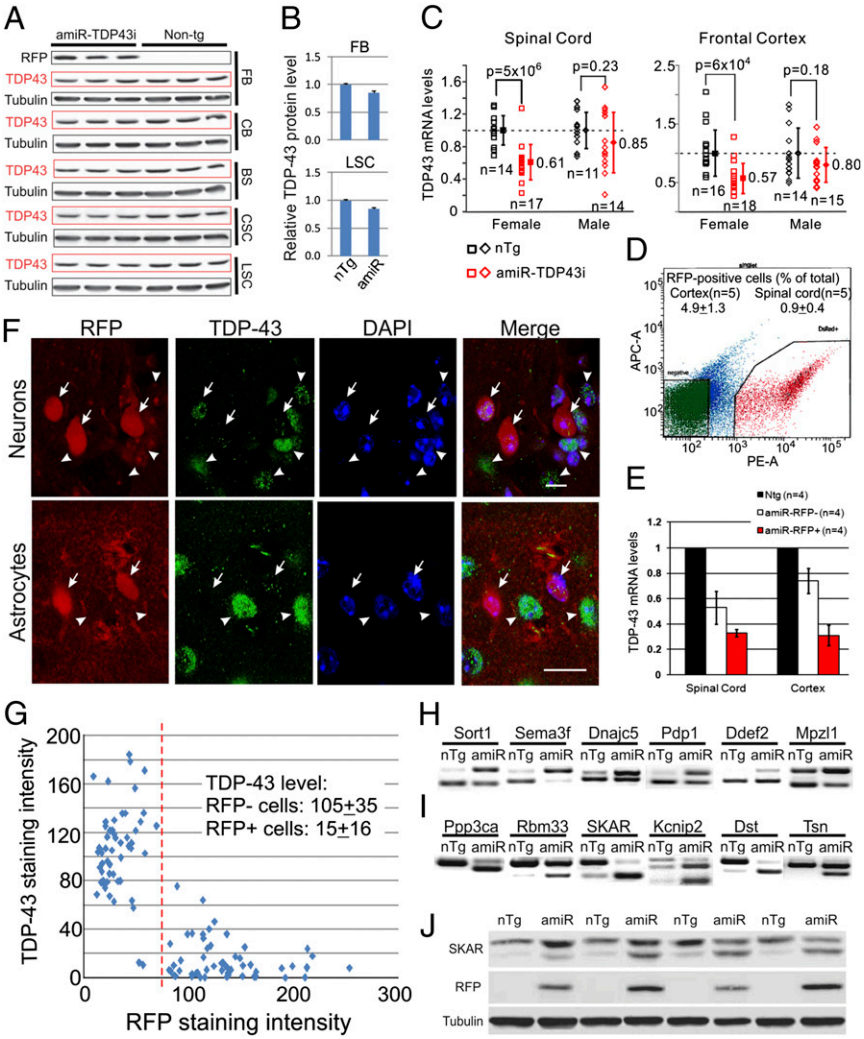

Fig. 2. The TDP-43 level and function were reduced in the amiR–TDP43i mice. (*A*) A modest knockdown of TDP-43 protein in forebrain (FB), cerebellum (CB), brainstem (BS), cervical spinal cord (CSC), and lumbar spinal cord (LSC). (*B*) Quantification of TDP-43 protein in *A* in FB (*Upper*) and LSC (*Lower*). All other areas had a similar decrease of ∼10% compared with the nTg mice. For values and statistics, see *SI Appendix*, Table S6. (*C*) TDP-43 mRNA was knocked down in amiR–TDP43i mice (red symbols) compared with nTg mice (black symbols). Each open symbol represents quantitative PCR (qPCR) of the mRNA from a single animal. The filled symbols represent the average. Error bars are SD. P values are derived by Student *t* test comparing the amiR–TDP43i with the nTg mice. (*D*) The RFP-positive (red area) and RFP-negative (green area) cells were sorted and collected from the cortex or spinal cord of the amiR–TDP43i mice. The average percentage of RFP-positive cells from the cortex and spinal cord are indicated in the graph. Notice that only low percentage of cells was collected as RFP-positive cells. The RFP-negative cells were also collected from nTg mice by using the same sorting procedure and were used as control. (*E*) TDP-43 mRNA levels in the sorted cells were measured by using qPCR. (*F*) Double immunofluorescent staining of RFP and TDP-43 in the cortex of amiR–TDP43i mice. Notice that TDP-43 staining was weaker in RFP-positive cells (arrows) than in the RFP-negative cells (arrowheads). (Scale bars: 10 μm.) (*G*) TDP-43 staining intensity was quantified from the cortices stained for RFP and TDP-43. Notice an inverse correlation between the TDP-43 and the RFP staining intensities (in arbitrary units). The average TDP-43 signal with SDs of the RFP-negative cells (to the left of the dotted line) and the RFP-positive cells (to the right of the dotted line) is shown. (*H*) Examples of increased exon inclusion (the increased levels in the upper band) in the TDP-43–regulated genes measured from the total RNA prepared from the RFP-positive cells from the frontal cortex of amiR–TDP43i mice. PCR was conducted by using the primer pairs against each target gene across the alternatively spliced exon. (*I*) Examples of increased exon exclusion (the increased levels in the lower band) measured from the same samples as in *H*. The same changes were also observed in the sorted cells from the spinal cord. (*J*) Western blot of the SKAR protein in the spinal cord homogenates. In all of the four amiR–TDP43i mice (amiR), the lower band that represented the isoform with exon 3 exclusion was increased. The same exact pattern was observed from the cortical homogenates.

To further characterize the pattern of TDP-43 knockdown in the spinal cord, we stained spinal cord sections for TDP-43 and choline acetyltransferase (ChAT) or TDP-43 and GFAP (Fig. 3 *A* and *B*). Nearly all ChAT-positive motor neurons and the GFAP-positive astrocytes were RFP-positive in the amiR–TDP43i mice (*SI Appendix*, Fig. S7). Therefore, we compared the TDP-43 fluorescence intensity in the ChAT- or GFAP-positive cells between the amiR–TDP43i and nTg mice. We found a significantly lowered level of TDP-43 in astrocytes, but not in motor neurons in the amiR–TDP43i mice (Fig. 3 *A*–*C*). The lack of detectable knockdown in motor neurons was likely a result of relatively weak transgene expression in motor neurons compared with the astrocytes (Fig. 3*D*). Thus, the transgene expression and TDP-43 knockdown predominantly occur in astrocytes in the spinal cord.

Mice Expressing amiR–TDP43 Develop Neurodegeneration in Layer V Cortex and Ventral Horn Spinal Cord. Hyperactivity is a common phenotype in many rodent models of forebrain neurodegeneration (49–53). Therefore, the hyperactivity of the amiR–TDP43i mice suggested the presence of neuronal degeneration in the forebrain.

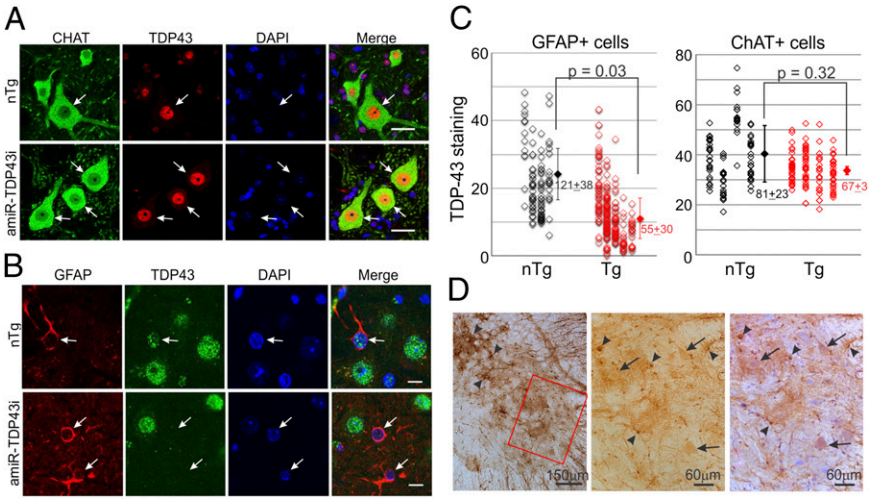

Fig. 3. TDP-43 was knocked down in astrocytes but not in motor neurons in the spinal cord. (*A*) Spinal cord sections from Tg and nTg animals were stained for ChAT and TDP-43. Notice the similar TDP-43 staining intensities in the motor neuron nuclei of the nTg and Tg mice (arrows). (*B*) Spinal cord sections were stained for GFAP and TDP-43. Notice the reduced TDP-43 staining intensity in the astrocytic nuclei compared with the nTg ones (arrows). (*C*) TDP-43 staining intensity was quantified in the GFAP-positive (*Left*) and ChAT-positive (*Right*) cells in the Tg and nTg mice. Each symbol represents the level in a single cell. Each column of symbols represents the levels from individual cells in one mouse. The averages from each animal were calculated, and the averages of animals from nTg and Tg were further calculated from the averages of individual animals. The values from Tg and nTg groups were then compared by using Student's *t* test. (*D*) Immunohistochemical staining for RFP in the spinal cord of amiR–TDP43i mice. The ventral horn area (red box) in *Left* was enlarged in *Center*, which showed that the overall staining intensity in the motor neurons (arrows) was lower than in the astrocytes (arrowheads). *Right* was the same as *Center* but was counterstained with hematoxylin.

Indeed, we detected a significantly reduced brain mass compared with controls (Fig. 4*A*) and robust astrogliosis in the deep layer of the frontal cortex (Fig. 4*B*). A quantitative analysis of the cortex using Nissl-stained sections revealed an ∼25% loss of large neurons in cortical layer V (Fig. 4 *C*–*E*).

The motor weakness and paralysis suggested the presence of motor neuron degeneration. To confirm this possibility, we examined the spinal cord of the amiR–TDP43i mice. We observed abundant astrogliosis and microgliosis in the ventral horn gray matter (*SI Appendix*, Fig. S8*A*). Additionally, at the paralysis stage there was an elevation in the expression of lipocalin 2, a factor that is induced in reactive astrocytes and is toxic to neurons (54) (*SI Appendix*, Fig. S8*B*). Furthermore, ChAT staining revealed dramatic motor neuron loss in the amiR–TDP43i mice (Fig. 5 *A* and *B*), which showed ∼60% fewer motor neurons in the ventral horn compared with the nTg mice (Fig. 5*C*). Because TDP-43 knockdown can lower ChAT expression (46), to rule out the possibility that a reduced ChAT expression rather than an actual motor neuron loss accounted for the reduced motor neuron numbers, we analyzed the spinal cord nerve roots. There was an age-dependent and selective degeneration of axons in the ventral but not in the dorsal roots (Fig. 5 *D* and *E*). This selectivity was not due to a lack of transgene expression in neurons in the dorsal root ganglia because the RFP expression could be readily detected in the dorsal root ganglia (*SI Appendix*, Fig. S8*C*).

A consequence of motor axon degeneration is denervation atrophy of skeletal muscles and compensatory hypertrophy of some muscle fibers. Data from our needle EMG measurements were consistent with the presence of active denervation (Fig. 1*F* and *SI Appendix*, Table S3). To confirm this morphologically, we examined the skeletal muscle. We noticed necrotic muscle fibers and fibers with centralized nuclei in some areas of the muscle (*SI Appendix*, Fig. S8*D*). These changes were likely caused by the transgene expression and TDP-43 knockdown in the muscle (*SI Appendix*, Fig. S8*E*). Nevertheless, both atrophic and hypertrophic muscle fibers that are characteristic of partially denervated muscle were readily observed (*SI Appendix*, Fig. S8*D*), thus confirming the presence of muscle denervation.

Evidence for TDP-43 Dysfunction in Human ALS Spinal Cords. Our data demonstrate that a partial loss of TDP-43 function can cause neurodegeneration and motor neuron disease phenotypes. This raises the question of whether TDP-43 dysfunction occurs in human ALS. To address this question, we selected 11 alternatively spliced genes that are highly regulated by TDP-43 (46, 48) and measured their changes in human cells after TDP-43 knockdown and overexpression for verification (*SI Appendix*, Fig. S9 *A*–*C*). We found one gene (REEP6) that did not display any changes in its alternative splicing under either knockdown or overexpression conditions. Another gene (EIF4H) increased the exon-inclusion product after TDP-43 knockdown but did not change significantly after TDP-43 overexpression. The majority (7 of 11) displayed changes in opposite directions between the knockdown and overexpression, indicating that changes in the alternative splicing of these genes reflect the changes in TDP-43 function (a reduction or an enhancement). Surprisingly, two genes displayed changes in the same direction after TDP-43 knockdown or overexpression (*SI Appendix*, Fig. S9*C*). Based on these results, we selected the 10 genes whose changes were verified in these assays and measured their splicing changes in human ALS and control spinal cords. We found that 6 of 10 genes did not show significant changes (*SI Appendix*, Fig. S9*D*). Among the remaining four genes, one (RWDD1) showed change consistent with an enhancement in TDP-43 function, two (RABGEF1 and EIF4H) showed changes consistent with a reduction in TDP-43 function, and one (POLDIP3) showed change consistent with both enhancement and reduction in TDP-43 function (Fig. 6). These results suggest that TDP-43 functions are altered in human ALS.

Discussion

TDP-43 aggregation accompanied by its nuclear depletion is involved in >95% of ALS and 40% of FTLD cases (6, 10). In some ALS cases, TDP-43 proteinopathy and nuclear depletion are caused by mutations in the TDP-43 gene (7, 8). Although these are rare (<1%) FALS cases, the presence of the same kind of TDP-43 pathology in these FALS cases and the more common cases—including the majority of FALS cases with non–TDP-43

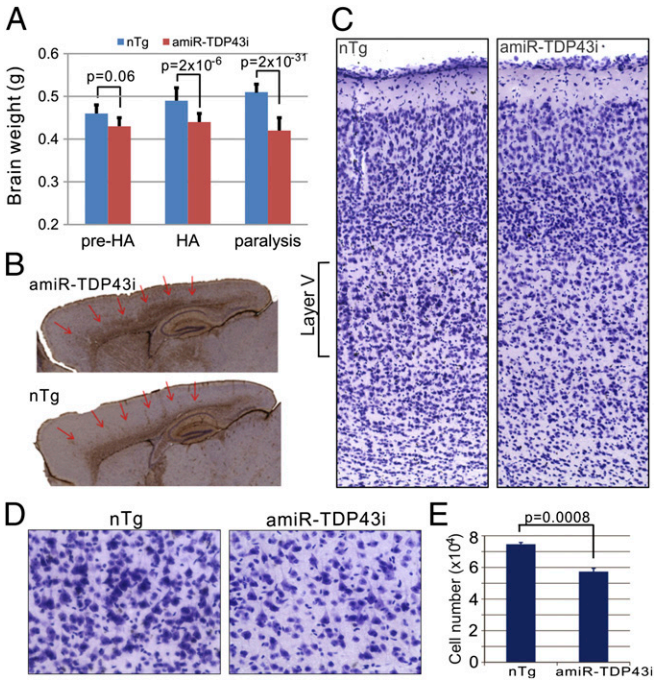

Fig. 4. The amiR–TDP43i mice developed cortical neuronal degeneration. (*A*) The brain weight in the amiR–TDP43i mice was significantly lower than the control nTg mice starting from the HA (hyperactive) stage. Eleven or more mice in each group were averaged and compared. (*B*) Astrogliosis developed in the deep layer of the cortex (arrows) in the amiR–TDP43i mice compared with the nTg control. The sections were stained for GFAP. (*C*) Loss of layer V long projecting neurons in the cortex of amiR–TDP43i mice. (*D*) Higher magnification of layer V in the nTg and amiR–TDP43i mice showing a reduced number of large neurons in the amiR–TDP43i mice. (*E*) Approximately 25% of large neurons were lost in the amiR–TDP43i mice (n = 3 in each group).

mutations and the sporadic cases (55–57)—suggests that these ALS populations share the same pathogenic pathway, albeit the origination of the pathogenesis differs. However, the significance of neither the aggregation nor the nuclear depletion is known. Although the aggregation is postulated to generate cellular toxicity, the aggregation with its accompanying nuclear depletion of TDP-43 could also decrease the functional TDP-43, thus causing a partial loss of TDP-43 function. This raises the question of whether a partial loss of TDP-43 function causes motor neuron degeneration and ALS. We have addressed this question by knocking down TDP-43 using RNAi in the amiR–TDP43i Tg mouse model. Our studies have unequivocally demonstrated that this model had a partial loss of TDP-43 function (Figs. 2 and 3) and developed motor neuron degeneration and ALS symptoms (Figs. 1, 4, and 5).

Did the partial loss of TDP-43 cause motor neuron degeneration and ALS symptoms in the amiR–TDP43i model? To answer this question, we need to consider several possible sources of artifacts. First, the motor neuron degeneration might be caused by disruption of a vital endogenous gene from the transgene insertion. This possibility has been ruled out because the uninduced transgene amiR–TDP43u that was inserted into the same genomic location did not cause the disease. Second, the motor neuron degeneration might be caused by overexpression of exogenous miRNA, which overwhelmed the endogenous miRNA processing machinery and thereby interfered with the endogenous miRNA generation, or evoked off-target silencing of other genes (58, 59). The best approach to rule out these possibilities is a rescue experiment, in which a TDP-43 gene that contains silent mutations in the amiR-TDP43 target region and is resistant to the RNAi mediated by the amiR–TDP43 is overexpressed to compensate for the lost TDP-43. However, this approach is impractical for several reasons. Overexpression of wild-type TDP-43 can generate toxicity and motor neuron degeneration (15). Even if Tg lines with low levels of overexpression may be obtained and thereby the neurodegeneration avoided, it would be difficult to know whether the expression level is sufficient for the rescue, and it would be impossible to guarantee that TDP-43 is overexpressed in the same cells where the amiR-TDP43 is expressed. Notwithstanding the absence of the rescue experiment, it is unlikely that a nonspecific effect caused the motor neuron degeneration and ALS phenotype because such an effect is observed only in extremely high levels of siRNA or shRNA expression conditions (58, 59). In the amiR–TDP43i mice, the amiR-TDP43 was produced at extremely modest levels in the CNS. By deep sequencing of the total miRNA from the cortices of three amiR–TDP43i mice, we found that the amiR–TDP43 comprised <1% of the highest endogenous miRNA reads and <0.1% of the total endogenous miRNA reads. Additionally, the mice expressing a scrambled amiRNA, the amiR-SCRi mice, did not develop any overt phenotypes (*SI Appendix*, Fig. S4). Therefore, it is likely that knockdown of TDP-43 caused motor neuron degeneration and ALS phenotype in the amiR–TDP43i mice.

Previous studies attempted to model loss of TDP-43 function by deletion of TDP-43 gene specifically in motor neurons (42, 43). Wu et al. reported that motor neuron-selective TDP-43 knockouts driven by HB9–Cre developed weakness and premature death (43). However, the evidence for motor neuron degeneration driving the phenotype was equivocal. The data did not clearly differentiate motor neuron atrophy or loss of ChAT expression from motor neuron death. Indeed, Iguchi et al. selectively deleted the TDP-43 gene from motor neurons using a VAChT–Cre driver (42). They observed motor neuron atrophy and dysfunction, but no motor neuron loss and premature death

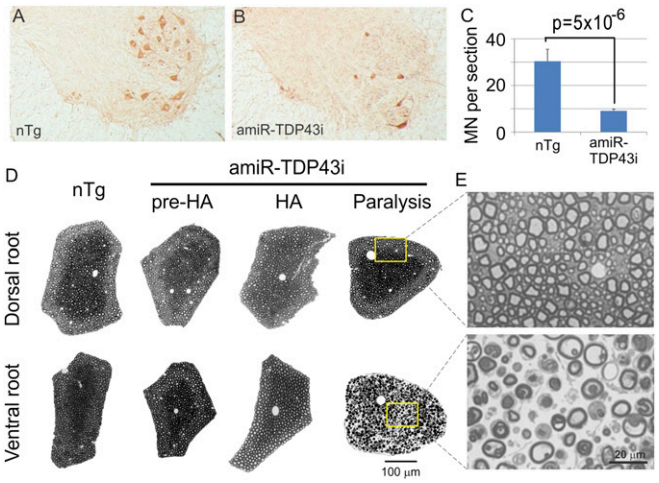

Fig. 5. Loss of spinal motor neurons in the amiR–TDP43i mice. (*A* and *B*) ChAT staining revealed dramatic loss of motor neurons in the ventral horn of the amiR–TDP43i mice. (*C*) Quantification of ChAT-positive cells in the spinal cord sections. ChAT-positive cells in the ventral horn were counted in 8–10 sections from the lumbar L4-5 levels of each animal. The average number per section was calculated from each animal. The numbers from four amiR–TDP43i and eight nTg controls were further averaged and shown here. Error bars represent SD. (*D*) The motor axons in the ventral root were normal in prehyperactive (pre-HA) and hyperactive (HA) stages but were degenerating in the paralysis stage. In contrast, the sensory axons in the dorsal root remain normal throughout all stages. (*E*) High magnification of the boxed area in the dorsal and ventral root in at the paralysis stage revealed axon degeneration in the ventral but not in the dorsal roots.

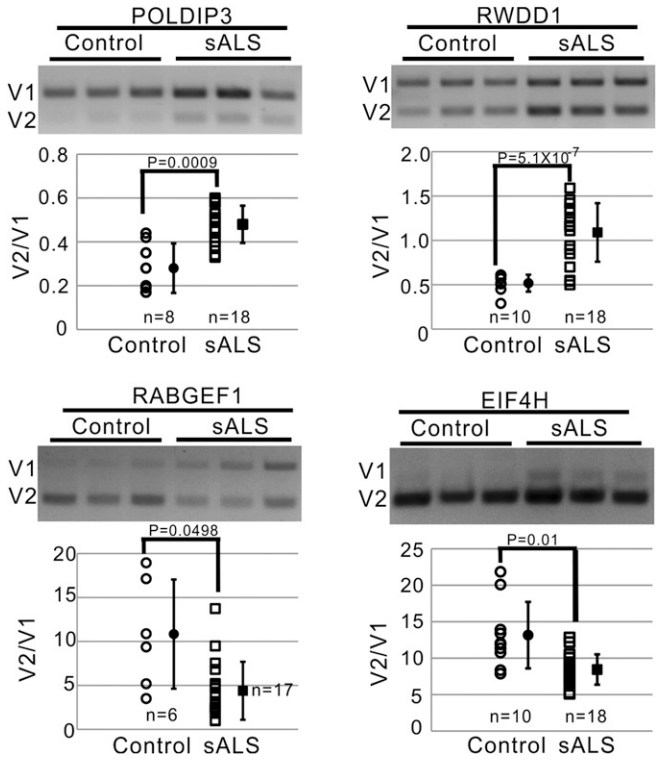

Fig. 6. Changes in alternative splicing detected in human ALS spinal cords. Three genes, Poldip3, Rabgef1, and Eif4h, changed in a pattern that is consistent with reduced TDP-43 function in ALS spinal cords. One gene, RWDD1, changed in a pattern that is opposite to the pattern induced by TDP-43 knockdown. V1, the exon-included variant; V2, the exon-excluded variant.

of the animals. Compared with these motor neuron-specific TDP-43 knockout mice, the amiR–TDP43i mice appeared to have developed more devastating motor neuron loss and clinical phenotypes (Figs. 1–5). This severe level of motor neuron loss in the knockdown mice cannot be explained by the degree of TDP-43 loss in the motor neurons because motor neurons completely lack TDP-43 in the knockout mice but have apparently normal levels in the amiR–TDP43i mice (Fig. 3). Instead, the reduced levels of TDP-43 function in astrocytes may play a key role (Fig. 3). Thus, our data, in conjunction with the data from Iguchi et al., suggest that TDP-43 dysfunction in glial cells plays a critical role in driving motor neuron death.

This conclusion is consistent with the strengthening notion that glia participate in driving motor neuron degeneration in ALS. Expression of mutant Cu/Zn superoxide dismutase (SOD1), the first identified ALS-causing gene mutation, in both motor neurons and glia, which include astrocytes and oligodendrocytes, drive motor neuron degeneration and ALS phenotype in the mutant SOD1 Tg mice (60, 61). Mutant SOD1 expression in astrocytes causes these cells to produce and secrete toxic factors that kill motor neurons (54, 62, 63). Transplanting astrocytes that express mutant SOD1 in wild-type animals causes motor neuron death (64). Recent evidence also supports an important role of astrocytes in TDP-43–mediated motor neuron toxicity. Overexpression of mutant TDP-43 in astrocytes causes motor neuron degeneration in vivo (65). Although mutant TDP-43 expression in motor neurons is sufficient to induce motor neuron death (66), astrocytes participate in this process by responding to signals from motor neurons and producing and secreting neurotoxic factor lipocalin 2 (54), which was also elevated in the amiR–TDP43i mice (*SI Appendix*, Fig. S8*B*). The demonstration that astrocytes derived from neural stem cells from sporadic ALS patients, but not those from normal controls, mediated motor neuron toxicity suggests that astrocytes participate in pathogenesis of ALS (67). Notably, TDP-43 aggregates in both motor neurons and glial cells are a general hallmark in sporadic ALS (28, 29, 68–70). Together, our results suggest that TDP-43 dysfunction in glial cells contributes to motor neuron degeneration in ALS.

In the amiR–TDP43i mice, TDP-43 was knocked down in muscles, and there was muscle degeneration in addition to changes typical of denervation atrophy (*SI Appendix*, Fig. S8*D*). Therefore, it is possible that the muscle degeneration contributed to motor neuron dysfunction and degeneration. It has been reported that muscle degeneration can cause denervation and some degenerative changes in motor neurons, including axon terminal degeneration and microgliosis in the spinal cord (71–73). However, most studies also demonstrate that muscle degeneration is not a primary driver for motor neuron death to the degree observed in ALS (71, 72, 74, 75). Although one study suggested that mutant SOD1 expressed in muscles could drive motor neuron loss (73), the evidence was equivocal and inconsistent with the conclusions of other studies. Thus, although the muscle degeneration might have contributed to the denervation and the overall neuromuscular phenotype, it is unlikely the driver for the motor neuron death in the CNS in amiR–TDP43i mice.

Given the broad expression of the amiR–TDP43 (*SI Appendix*, Figs. S5 and S6), it is striking that the predominant phenotype in the amiR–TDP43i mice is neurological (Fig. 1) and the predominant neuronal loss is concentrated in the large neurons with long projecting axons—i.e., the cortical layer V pyramidal neurons and spinal cord motor neurons (Figs. 4 and 5). Therefore, the key phenotypes and pathology in the amiR–TDP43i mice have replicated the core features of ALS, thus suggesting that the large neurons in the motor system of the CNS possess a heightened vulnerability to TDP-43 dysfunction relative to other cell types and that TDP-43 dysfunction plays a role in ALS.

Therefore, to explore whether TDP-43 dysfunction exists in humans, we evaluated TDP-43 function by measuring alternative splicing changes in the TDP-43–regulated genes. We have detected changes that are consistent with both an enhancement in TDP-43 function in some genes and a decrease in TDP-43 function in others (Fig. 6). These findings suggest that TDP-43 function is altered in ALS. However, why most of the TDP-43 target genes remain unchanged, and those changed are simultaneously in the direction of an enhancement and a decrease in TDP-43 function, remains a conundrum. The fact that most of the target genes remain unchanged indicates that the signal for TDP-43 dysfunction is small. A possible scenario that results in a small overall change in TDP-43 function could be that the TDP-43 dysfunction develops gradually, and at each point in time only a minority of the cell populations has ongoing TDP-43 dysfunction. The observation that the human ALS tissue simultaneously display signals for an increase and a decrease of TDP-43 function could be a reflection of a complex state of TDP-43 function in ALS. It has been well established that the TDP-43 level is normally maintained constant by an autoregulatory mechanism (46, 76), and the observed alterations in alternative splicing may reflect a state of TDP-43 deregulation and dysfunction, which could have a major role in motor neuron degeneration and ALS phenotypes. Indeed it has been reported that TDP-43 levels in human ALS is modestly elevated (16, 77). Because TDP-43 functions in multiprotein/RNA complexes, an elevation in the TDP-43 level could disrupt the stoichiometry among the components in the complex, thereby causing dysfunction of the TDP-43 complexes (13). However, it remains to be investigated how functions of TDP-43 complexes change under modestly but persistently elevated TDP-43 levels. In complex tissues such as the CNS, the functional changes measured from total spinal cord RNA reflect averages from different cell populations, which

could also vary at different stages of neurodegeneration. The complexity of this condition could thereby produce varied changes in alternative splicing. For example, an elevated TDP-43 level in one cell population might enhance, whereas in another might inhibit, its normal function. It may also be possible that an elevated TDP-43 level initially enhances its function, but when the elevation exceeds a certain threshold at a late disease stage, an inhibition develops. Therefore, our results call for further investigation on the alterations in the TDP-43 levels and function in model systems for ALS and in human ALS tissues.

Materials and Methods

Tg Mice. The transgene amiR–TDP43u was built by using our published method (78). The preamiR-TDP43b sequence (21) was inserted into the pCAG-GFP/RFP-miRint-KX (78) (Addgene no. 19818). This transgene was a conditional construct that initially expressed GFP, but in the presence of Cre, the GFP sequence would be excised and the CAG promoter would drive expression of RFP and the amiR–TDP43 (*SI Appendix*, Fig. S1*A*). The Tg lines were created and screened as described (45). An artifact associated with multiple transgene integration into the mouse genome precluded a selective induction of transgene expression in the CNS (45) (*SI Appendix*, Fig. S1 *B* and *C*). Therefore, a GFP-expressing Tg line was converted to a line that constitutively and ubiquitously expressed RFP and amiR–TDP43 (*SI Appendix*, Figs. S1*D* and S2). As a control, a Tg line that constitutively expressed RFP and a scrambled amiRNA that does not target any known mouse genes (amiR-SCR) was also established. See details in *SI Appendix, SI Materials and Methods*. The preinduction parent Tg line (amiR–TDP43u or CAG-loxp-EGFP/3xpA-loxp-RFP-amiR-TDP43 mice) will be available from The Jackson Laboratory as stock no. 017919. The post-induction line (amiR–TDP43i mice) will be available from The Jackson Laboratory as stock no. 017934.

Behavioral Analysis and EMG. All mice were maintained at the University of Massachusetts Medical School animal facility according to the guidelines set forth by the Institutional Animal Care and Use Committee (IACUC), and all animal procedures were approved by the IACUC. The mice were maintained in pathogen-free environment and on a 12-h light-dark cycle. The Tg mice were monitored daily for their appearance and motor activity. They were weighed once or twice weekly. Their motor behavior was monitored at different disease stages by using an automated video monitoring system. Their muscle activity was monitored by EMG. See details in *SI Appendix, SI Materials and Methods*.

Measurement of Transgene Expression and TDP-43 Knockdown. Transgene expression was measured in tissue homogenates by immunoblots for GFP and RFP and by Northern blots for amiR–TDP43. The tissue expression pattern was determined by immunohistochemistry of brain and spinal cord sections. TDP-43 knockdown was measured in tissue homogenates and RFP-positive cells sorted from the cortex and the spinal cord by using immunoblots and reverse-transcriptase quantitative PCR. See details in *SI Appendix, SI Materials and Methods*.

Visualization and Quantification of Neurodegeneration. The sagittal sections from the whole mouse brains were visualized by Nissl staining. Layer V pyramidal neurons were quantified by using Stereo Investigator software (MBF Bioscience). Spinal cord motor neurons were visualized by staining for ChAT, and the ChAT-positive cells were counted. Ventral root axons were visualized by cross-sections of L4 and L5 nerve roots stained with toluidine blue. Skeletal muscle morphology was visualized by cross-sectioned gastrocnemius muscle stained with hematoxylin & eosin. See details in *SI Appendix, SI Materials and Methods*.

Measurement of Alternative Splicing in Human Cells and Spinal Cord. Total RNA was extracted from human cells transfected with plasmid expressing TDP-43 or with siRNA targeting TDP-43 for knockdown. The alternative splicing was assayed by PCR using primers across the alternatively spliced exons. The PCR products were resolved on agarose gels, and the bands were quantified to determine the relative ratios of the exon-excluded band to the exon included band. See details in *SI Appendix, SI Materials and Methods*.

Statistics. Quantitative data on TDP-43 knockdown and pathology in amiR–TDP43i mice were compared with those from the nTg mice by using Student's *t* test. Genotype frequencies were compared by using the χ^2 test.

ACKNOWLEDGMENTS. We thank Drs. Jemeen Sreedharan and Daryl Bosco for critically reading the manuscript; Drs. Alonzo Ross and Phillip D. Zamore for sharing equipment; Dr. Hong Cao for assisting with confocal imaging; the UMass Transgenic Animal Modeling Core for pronuclear injection; and the technical support from the Core Electron Microscopy Facility, which receives support from the National Center for Research Resources (S10RR027897). This work was supported by National Institutes of Health/National Institute of Neurological Disorders and Stroke Grants R21NS062230 and R01NS059708, the ALS Association, ALS Therapeutic Alliance, and the Packard Center for ALS Research at Johns Hopkins (to Z.X.); and in part by National Institute on Aging/National Institutes of Health Intramural Research Program AG000943.

1. Ling SC, et al. (2010) ALS-associated mutations in TDP-43 increase its stability and promote TDP-43 complexes with FUS/TLS. *Proc Natl Acad Sci USA* 107(30):13318–13323.
2. Sephton CF, et al. (2011) Identification of neuronal RNA targets of TDP-43-containing ribonucleoprotein complexes. *J Biol Chem* 286(2):1204–1215.
3. Kim SH, Shanware NP, Bowler MJ, Tibbetts RS (2010) Amyotrophic lateral sclerosis-associated proteins TDP-43 and FUS/TLS function in a common biochemical complex to co-regulate HDAC6 mRNA. *J Biol Chem* 285(44):34097–34105.
4. Freibaum BD, Chitta RK, High AA, Taylor JP (2010) Global analysis of TDP-43 interacting proteins reveals strong association with RNA splicing and translation machinery. *J Proteome Res* 9(2):1104–1120.
5. Buratti E, Baralle FE (2010) The multiple roles of TDP-43 in pre-mRNA processing and gene expression regulation. *RNA Biol* 7(4):420–429.
6. Ling SC, Polymenidou M, Cleveland DW (2013) Converging mechanisms in ALS and FTD: Disrupted RNA and protein homeostasis. *Neuron* 79(3):416–438.
7. Sreedharan J, et al. (2008) TDP-43 mutations in familial and sporadic amyotrophic lateral sclerosis. *Science* 319(5870):1668–1672.
8. Kabashi E, et al. (2008) TARDBP mutations in individuals with sporadic and familial amyotrophic lateral sclerosis. *Nat Genet* 40(5):572–574.
9. Robberecht W, Philips T (2013) The changing scene of amyotrophic lateral sclerosis. *Nat Rev Neurosci* 14(4):248–264.
10. Mackenzie IRA, Rademakers R, Neumann M (2010) TDP-43 and FUS in amyotrophic lateral sclerosis and frontotemporal dementia. *Lancet Neurol* 9(10):995–1007.
11. Smith DH, Johnson VE, Stewart W (2013) Chronic neuropathologies of single and repetitive TBI: Substrates of dementia? *Nat Rev Neurol* 9(4):211–221.
12. Lee EB, Lee VMY, Trojanowski JQ (2012) Gains or losses: Molecular mechanisms of TDP43-mediated neurodegeneration. *Nat Rev Neurosci* 13(1):38–50.
13. Xu ZS (2012) Does a loss of TDP-43 function cause neurodegeneration? *Mol Neurodegener* 7(1):27.
14. Halliday G, et al. (2012) Mechanisms of disease in frontotemporal lobar degeneration: Gain of function versus loss of function effects. *Acta Neuropathol* 124(3):373–382.
15. Tsao W, et al. (2012) Rodent models of TDP-43: Recent advances. *Brain Res* 1462(0): 26–39.
16. Gitcho MA, et al. (2009) TARDBP 3′-UTR variant in autopsy-confirmed frontotemporal lobar degeneration with TDP-43 proteinopathy. *Acta Neuropathol* 118(5):633–645.
17. Swarup V, et al. (2011) Pathological hallmarks of amyotrophic lateral sclerosis/frontotemporal lobar degeneration in transgenic mice produced with TDP-43 genomic fragments. *Brain* 134(Pt 9):2610–2626.
18. Watanabe S, Kaneko K, Yamanaka K (2013) Accelerated disease onset with stabilized familial amyotrophic lateral sclerosis (ALS)-linked mutant TDP-43 proteins. *J Biol Chem* 288(5):3641–3654.
19. Polymenidou M, Cleveland DW (2011) The seeds of neurodegeneration: Prion-like spreading in ALS. *Cell* 147(3):498–508.
20. Johnson BS, et al. (2009) TDP-43 is intrinsically aggregation-prone, and amyotrophic lateral sclerosis-linked mutations accelerate aggregation and increase toxicity. *J Biol Chem* 284(30):20329–20339.
21. Yang C, et al. (2010) The C-terminal TDP-43 fragments have a high aggregation propensity and harm neurons by a dominant-negative mechanism. *PLoS ONE* 5(12): e15878.
22. Guo W, et al. (2011) An ALS-associated mutation affecting TDP-43 enhances protein aggregation, fibril formation and neurotoxicity. *Nat Struct Mol Biol* 18(7):822–830.
23. Wegorzewska I, Bell S, Cairns NJ, Miller TM, Baloh RH (2009) TDP-43 mutant transgenic mice develop features of ALS and frontotemporal lobar degeneration. *Proc Natl Acad Sci USA* 106(44):18809–18814.
24. Zhou H, et al. (2010) Transgenic rat model of neurodegeneration caused by mutation in the TDP gene. *PLoS Genet* 6(3):e1000887.
25. Arnold ES, et al. (2013) ALS-linked TDP-43 mutations produce aberrant RNA splicing and adult-onset motor neuron disease without aggregation or loss of nuclear TDP-43. *Proc Natl Acad Sci USA* 110(8):E736–E745.
26. Barmada SJ, et al. (2010) Cytoplasmic mislocalization of TDP-43 is toxic to neurons and enhanced by a mutation associated with familial amyotrophic lateral sclerosis. *J Neurosci* 30(2):639–649.
27. Estes PS, et al. (2011) Wild-type and A315T mutant TDP-43 exert differential neurotoxicity in a Drosophila model of ALS. *Hum Mol Genet* 20(12):2308–2321.
28. Arai T, et al. (2006) TDP-43 is a component of ubiquitin-positive tau-negative inclusions in frontotemporal lobar degeneration and amyotrophic lateral sclerosis. *Biochem Biophys Res Commun* 351(3):602–611.
29. Neumann M, et al. (2006) Ubiquitinated TDP-43 in frontotemporal lobar degeneration and amyotrophic lateral sclerosis. *Science* 314(5796):130–133.

30. Shiga A, et al. (2012) Alteration of POLDIP3 splicing associated with loss of function of TDP-43 in tissues affected with ALS. *PLoS ONE* 7(8):e43120.
31. Schmid B, et al. (2013) Loss of ALS-associated TDP-43 in zebrafish causes muscle degeneration, vascular dysfunction, and reduced motor neuron axon outgrowth. *Proc Natl Acad Sci USA* 110(13):4986–4991.
32. Fiesel FC, Schurr C, Weber SS, Kahle PJ (2011) TDP-43 knockdown impairs neurite outgrowth dependent on its target histone deacetylase 6. *Mol Neurodegener* 6:64.
33. Iguchi Y, et al. (2009) TDP-43 depletion induces neuronal cell damage through dysregulation of Rho family GTPases. *J Biol Chem* 284(33):22059–22066.
34. Lu Y, Ferris J, Gao FB (2009) Frontotemporal dementia and amyotrophic lateral sclerosis-associated disease protein TDP-43 promotes dendritic branching. *Mol Brain* 2:30.
35. Godena VK, et al. (2011) TDP-43 regulates Drosophila neuromuscular junctions growth by modulating Futsch/MAP1B levels and synaptic microtubules organization. *PLoS ONE* 6(3):e17808.
36. Kabashi E, et al. (2010) Gain and loss of function of ALS-related mutations of TARDBP (TDP-43) cause motor deficits in vivo. *Hum Mol Genet* 19(4):671–683.
37. Vanden Broeck L, et al. (2013) TDP-43 loss-of-function causes neuronal loss due to defective steroid receptor-mediated gene program switching in Drosophila. *Cell Rep* 3(1):160–172.
38. Chiang P-M, et al. (2010) Deletion of TDP-43 down-regulates Tbc1d1, a gene linked to obesity, and alters body fat metabolism. *Proc Natl Acad Sci USA* 10(37):16320–16324.
39. Kraemer BC, et al. (2010) Loss of murine TDP-43 disrupts motor function and plays an essential role in embryogenesis. *Acta Neuropathol* 119(4):409–419.
40. Sephton CF, et al. (2010) TDP-43 is a developmentally regulated protein essential for early embryonic development. *J Biol Chem* 285(9):6826–6834.
41. Wu L-S, et al. (2010) TDP-43, a neuro-pathosignature factor, is essential for early mouse embryogenesis. *Genesis* 48(1):56–62.
42. Iguchi Y, et al. (2013) Loss of TDP-43 causes age-dependent progressive motor neuron degeneration. *Brain* 136(Pt 5):1371–1382.
43. Wu L-S, Cheng W-C, Shen CK (2012) Targeted depletion of TDP-43 expression in the spinal cord motor neurons leads to the development of amyotrophic lateral sclerosis-like phenotypes in mice. *J Biol Chem* 287(33):27335–27344.
44. Qiu L, Wang H, Xia X, Zhou H, Xu Z (2008) A construct with fluorescent indicators for conditional expression of miRNA. *BMC Biotechnol* 8(1):77.
45. Qiu L, Rivera-Pérez JA, Xu Z (2011) A non-specific effect associated with conditional transgene expression based on Cre-loxP strategy in mice. *PLoS ONE* 6(5):e18778.
46. Polymenidou M, et al. (2011) Long pre-mRNA depletion and RNA missplicing contribute to neuronal vulnerability from loss of TDP-43. *Nat Neurosci* 14(4):459–468.
47. Fiesel FC, Weber SS, Supper J, Zell A, Kahle PJ (2012) TDP-43 regulates global translational yield by splicing of exon junction complex component SKAR. *Nucleic Acids Res* 40(6):2668–2682.
48. Tollervey JR, et al. (2011) Characterizing the RNA targets and position-dependent splicing regulation by TDP-43. *Nat Neurosci* 14(4):452–458.
49. Unger EL, et al. (2006) Locomotor hyperactivity and alterations in dopamine neurotransmission are associated with overexpression of A53T mutant human alpha-synuclein in mice. *Neurobiol Dis* 21(2):431–443.
50. Lin X, et al. (2009) Leucine-rich repeat kinase 2 regulates the progression of neuropathology induced by Parkinson's-disease-related mutant alpha-synuclein. *Neuron* 64(6):807–827.
51. Steele AD, Jackson WS, King OD, Lindquist S (2007) The power of automated high-resolution behavior analysis revealed by its application to mouse models of Huntington's and prion diseases. *Proc Natl Acad Sci USA* 104(6):1983–1988.
52. Scattoni ML, et al. (2010) Early behavioural markers of disease in P301S tau transgenic mice. *Behav Brain Res* 208(1):250–257.
53. Musilli M, Nicolia V, Borrelli S, Scarpa S, Diana G (2013) Behavioral effects of Rho GTPase modulation in a model of Alzheimer's disease. *Behav Brain Res* 237:223–229.
54. Bi F, et al. (2013) Reactive astrocytes secrete lcn2 to promote neuron death. *Proc Natl Acad Sci USA* 110(10):4069–4074.
55. Van Deerlin VM, et al. (2008) TARDBP mutations in amyotrophic lateral sclerosis with TDP-43 neuropathology: A genetic and histopathological analysis. *Lancet Neurol* 7(5):409–416.
56. Yokoseki A, et al. (2008) TDP-43 mutation in familial amyotrophic lateral sclerosis. *Ann Neurol* 63(4):538–542.
57. Pamphlett R, Luquin N, McLean C, Jew SK, Adams L (2009) TDP-43 neuropathology is similar in sporadic amyotrophic lateral sclerosis with or without TDP-43 mutations. *Neuropathol Appl Neurobiol* 35(2):222–225.
58. Grimm D, et al. (2006) Fatality in mice due to oversaturation of cellular microRNA/short hairpin RNA pathways. *Nature* 441(7092):537–541.
59. Jackson AL, et al. (2006) Widespread siRNA "off-target" transcript silencing mediated by seed region sequence complementarity. *RNA* 12(7):1179–1187.
60. Ilieva H, Polymenidou M, Cleveland DW (2009) Non-cell autonomous toxicity in neurodegenerative disorders: ALS and beyond. *J Cell Biol* 187(6):761–772.
61. Lee Y, et al. (2012) Oligodendroglia metabolically support axons and contribute to neurodegeneration. *Nature* 487(7408):443–448.
62. Di Giorgio FP, Carrasco MA, Siao MC, Maniatis T, Eggan K (2007) Non-cell autonomous effect of glia on motor neurons in an embryonic stem cell-based ALS model. *Nat Neurosci* 10(5):608–614.
63. Nagai M, et al. (2007) Astrocytes expressing ALS-linked mutated SOD1 release factors selectively toxic to motor neurons. *Nat Neurosci* 10(5):615–622.
64. Papadeas ST, Kraig SE, O'Banion C, Lepore AC, Maragakis NJ (2011) Astrocytes carrying the superoxide dismutase 1 (SOD1G93A) mutation induce wild-type motor neuron degeneration in vivo. *Proc Natl Acad Sci USA* 108(43):17803–17808.
65. Tong J, et al. (2013) Expression of ALS-linked TDP-43 mutant in astrocytes causes non-cell-autonomous motor neuron death in rats. *EMBO J* 32(13):1917–1926.
66. Huang C, Tong J, Bi F, Zhou H, Xia XG (2012) Mutant TDP-43 in motor neurons promotes the onset and progression of ALS in rats. *J Clin Invest* 122(1):107–118.
67. Haidet-Phillips AM, et al. (2011) Astrocytes from familial and sporadic ALS patients are toxic to motor neurons. *Nat Biotechnol* 29(9):824–828.
68. Tan CF, et al. (2007) TDP-43 immunoreactivity in neuronal inclusions in familial amyotrophic lateral sclerosis with or without SOD1 gene mutation. *Acta Neuropathol* 113(5):535–542.
69. Hasegawa M, et al. (2008) Phosphorylated TDP-43 in frontotemporal lobar degeneration and amyotrophic lateral sclerosis. *Ann Neurol* 64(1):60–70.
70. Neumann M, et al. (2009) Phosphorylation of S409/410 of TDP-43 is a consistent feature in all sporadic and familial forms of TDP-43 proteinopathies. *Acta Neuropathol* 117(2):137–149.
71. Dobrowolny G, et al. (2008) Skeletal muscle is a primary target of SOD1G93A-mediated toxicity. *Cell Metab* 8(5):425–436.
72. Dupuis L, et al. (2009) Muscle mitochondrial uncoupling dismantles neuromuscular junction and triggers distal degeneration of motor neurons. *PLoS ONE* 4(4):e5390.
73. Wong M, Martin LJ (2010) Skeletal muscle-restricted expression of human SOD1 causes motor neuron degeneration in transgenic mice. *Hum Mol Genet* 19(11):2284–2302.
74. Miller TM, et al. (2006) Gene transfer demonstrates that muscle is not a primary target for non-cell-autonomous toxicity in familial amyotrophic lateral sclerosis. *Proc Natl Acad Sci USA* 103(51):19546–19551.
75. Da Cruz S, et al. (2012) Elevated PGC-1α activity sustains mitochondrial biogenesis and muscle function without extending survival in a mouse model of inherited ALS. *Cell Metab* 15(5):778–786.
76. Avendaño-Vázquez SE, et al. (2012) Autoregulation of TDP-43 mRNA levels involves interplay between transcription, splicing, and alternative polyA site selection. *Genes Dev* 26(15):1679–1684.
77. Swarup V, et al. (2011) Deregulation of TDP-43 in amyotrophic lateral sclerosis triggers nuclear factor κB-mediated pathogenic pathways. *J Exp Med* 208(12):2429–2447.
78. Yang C, Qiu L, Xu Z (2011) Specific gene silencing using RNAi in cell culture. *Methods Mol Biol* 793:457–477.